Reducing the Energy Demand of Corn-Based Fuel Ethanol Through Salt Extractive Distillation Enabled by Electrodialysis

Mohammed A. M. Hussain, Jennifer L. Anthony, and Peter H. Pfromm
Dept. of Chemical Engineering, Kansas State University, Manhattan, KS 66506

DOI 10.1002/aic.12577
Published online March 4, 2011 in Wiley Online Library (wileyonlinelibrary.com).

The thermal energy demand for producing fuel ethanol from the fermentation broth of a contemporary corn-to-fuel ethanol plant in the U.S. is largely satisfied by combustion of fossil fuels, which impacts the possible economical and environmental advantages of bioethanol over fossil fuels. To reduce the thermal energy demand for producing fuel ethanol, a process integrating salt extractive distillation—enabled by a new scheme of electrodialysis and spray drying for salt recovery—in the water-ethanol separation train of a contemporary corn-to-fuel ethanol plant is investigated. Process simulation using Aspen Plus® 2006.5, with the electrolyte nonrandom two liquid Redlich-Kwong property method to model the vapor liquid equilibrium of the water-ethanol-salt system, was carried out. The integrated salt extractive distillation process may provide a thermal energy savings of about 30%, when compared with the contemporary process for separating fuel ethanol from the beer column distillate. © 2011 American Institute of Chemical Engineers *AIChE J,* 58: 163–172, 2012

Keywords: salt extractive distillation, ethanol distillation, fuel ethanol, electrodialytic concentration, bioethanol

Introduction

Currently, the annual production capacity for fuel ethanol, mostly corn-ethanol, in the U.S. is about 55.7 GL, including about 4.5 GL capacity in new construction or expansion.[1] The Renewable Fuels Standard (RFS2), established under the Energy Independence and Security Act (EISA) of 2007, mandates the production of 136.3 GL/year of renewable fuels in 2022: 56.8 GL/year of corn-ethanol, 60.6 GL/year of second-generation bio-fuels such as cellulosic ethanol, and 18.9 GL/year of advanced bio-fuels such as biomass based diesel. Currently, dry milling is the most widely used process in the U.S for producing fuel ethanol from corn by fermentation. The energy demand of old dry mill facilities[2–8] was high. Contemporary dry mill facilities have higher energy efficiency and require about 9.8 MJ (generally from natural gas) of thermal energy and 0.7 MJ (0.19 kW h) of electrical energy to produce 1 liter of nondenatured fuel grade ethanol. The energy demand includes drying of nonfermentables to produce distillers' dried grain with solubles (DDGS).[9–12] The lower heating value of pure ethanol is 21.2 MJ per liter.[13] About 70% of the thermal energy is expended to generate steam which is used for recovering ethanol from fermentation broth, purifying ethanol to fuel grade (99.5 wt %), cooking and liquefying corn mash, and concentrating thin stillage. Recovering and purifying ethanol from fermentation broth is energy intensive and requires about 70% of the total steam generated in the dry milling plant.[14] Fuel ethanol plants mainly use natural gas boilers to generate steam. Reducing the steam demand for recovering and purifying ethanol is essential to improve the energy balance of bioethanol, even if nonfermentable biomass components

Correspondence concerning this article should be addressed to P. H. Pfromm at pfromm@ksu.edu.

would be burned instead of natural gas to produce steam. The vast amounts of bioethanol produced by fermentation worldwide would similarly benefit from reducing the energy demand of the water (fermentation broth)-ethanol separation.

The ethanol concentration in the fermentation broth may vary from about 10–15 wt % for different facilities.[10,15–18] The fermentation broth contains many components besides water and ethanol: unfermented biomass, microorganisms, proteins, oils, and volatile organics. Recovering ethanol from fermentation broth and purifying to fuel grade is difficult and energy intensive because of the dilute nature of the fermentation broth and the challenging water-ethanol vapor liquid equilibrium (VLE) with an azeotrope at about 96 wt % ethanol and tangential approach of the water-ethanol equilibrium curve to the 45° line at high ethanol concentrations in the familiar *y-x* VLE diagram representation. Simple distillation cannot be used to distill ethanol above the azeotropic composition. The state of the art technique used in the fuel ethanol industry to produce fuel ethanol is distillation close to the azeotropic composition followed by dehydration in a molecular sieve based adsorption unit[10,16,19,20] or, in some cases, distillation followed by dehydration with membrane vapor permeation.[15,21] Membrane-assisted vapor stripping was tested at the pilot scale level for producing fuel ethanol from a dilute ethanol feed (5 wt %), representing fermentation broth obtained from lignocellulosic feedstocks.[22,23] Green field facilities for producing fuel ethanol from lignocellulosic feedstocks are expected to be built to meet the requirements of EISA. Our study focuses on the significant installed capital equipment for corn-based fuel ethanol facilities where the ethanol concentration in the fermentation broth is much higher than is expected for the cellulosic case. The technology proposed here would offer retrofit opportunities for existing facilities, whereas the aforementioned membrane technology would be targeted towards new construction, not making use of the conventional equipment beyond the beer column. Membrane technology will, for example, require specialized ethanol vapor compressors. Heat integrated distillation operations such as multieffect distillation and vapor recompression can reduce distillation energy demand. In particular, multieffect distillation can lead to significant energy savings; 45% energy savings has been reported for a heat integrated dry mill process using multieffect distillation, compared with a heat integrated dry mill process using standard distillation.[24] Nevertheless, multieffect distillation is not considered in our study, as it requires a complete redesign of the distillation train of the existing dry mill corn-ethanol facilities.

The VLE of the water-ethanol system can be improved by employing a salt dissolved in the liquid phase to raise the equilibrium vapor ethanol content.[25–28] Adding a suitable salt can specifically improve the relative volatility of ethanol (“salting out”) as well as break the azeotrope.[25,27,29] For example, 99.6 wt % ethanol was distilled using potassium acetate as the salt with only a quarter of the energy required for salt-free distillation to obtain lower quality 93 wt % ethanol directly from a feed containing 70 wt % ethanol.[30] Efficient recovery and reuse of the salt used as the separating agent is, however, crucial.

Potassium acetate[29–37] and calcium chloride[31,36,38–40] have been reported for water-ethanol separation using the “salting out” effect. The use of the salt separating agent in a process with tightly closed water cycles such as the state of the art dry mill corn-to-fuel ethanol plant requires that the salt not impact other processing areas negatively. In this study, calcium chloride was selected for the following reasons: low cost, large “salting out” effect of calcium chloride,[31,36] and process compatibility. Calcium ion stabilizes the α-amylase enzyme,[41,42] used in the cooking process, and (at low levels) acts as a co-nutrient for yeast used in fermentation.[43]

In a salt extractive distillation column, the salt is usually dissolved in the reflux stream and introduced at the top of the column. Unlike the liquid extractive agents such as ethylene glycol, salt is nonvolatile and always remains in the liquid phase; thereby, enabling the production of a high purity distillate free of salt. The salt moves downward in the column and is recovered and purified from the distillation column bottoms for reuse in the top of the column. Hence, there are two distinct steps involved: salt extractive distillation and salt recovery/purification. Corrosion due to aqueous ethanolic salt solutions is an issue and special construction materials may be necessary or increased corrosion rates may be planned for.[38,44] Other issues are related to solids handling, feeding, and dissolving salt in the reflux stream, potential decrease in plate efficiency, and foaming inside the column.[25,27,29] In the study presented here, the possible benefit in terms of energy demand is established, which will determine if the concept is attractive enough to deal with the possible complications.

There are many experimental and theoretical studies[29–40] on producing fuel ethanol by using the “salting out” effect, but most of them focus only on the salt extractive distillation step. Moreover, the studies[25,27,32–35,37,38] which include both steps of salt extractive distillation and salt recovery do not consider techniques other than evaporation and drying for salt recovery. Evaporative salt concentration/crystallization and solids drying techniques are energy intensive. Reducing the energy demand for the salt recovery step becomes essential to reap the benefit of salt-induced VLE improvement. In this study, a combination of electrodialysis and spray drying is investigated. The salt extractive column bottoms stream is preconcentrated by electrodialysis and dried to an anhydrous state by spray drying. In electrodialysis, the dilute salt solution is concentrated by selectively separating the salt ions from the solution[45,46] rather than evaporating water; therefore, requiring less energy than that of an evaporative process. Moreover, electrodialysis is rugged and can be operated at high ionic strengths.[47] Final recovery of dry salt is achieved in a spray dryer. This approach is widely used to convert a liquid feed containing salt into dry solid particles in a single step.[48,49] Integrating salt extractive distillation, with salt recovery enabled by electrodialysis and spray drying, in the water-ethanol separation train of a state of the art corn-to-fuel ethanol plant was found to yield significant energy savings through process simulation using Aspen Plus® 2006.5.

Design Cases

Benchmark process: Case I

The target fuel ethanol production rate was set at 151.4 ML (1.17×10^5 tonne) per year with an ethanol concentration of 99.5 wt %. In a standard U.S. corn-to-fuel ethanol plant based on fermentation using yeast, recovery of ethanol

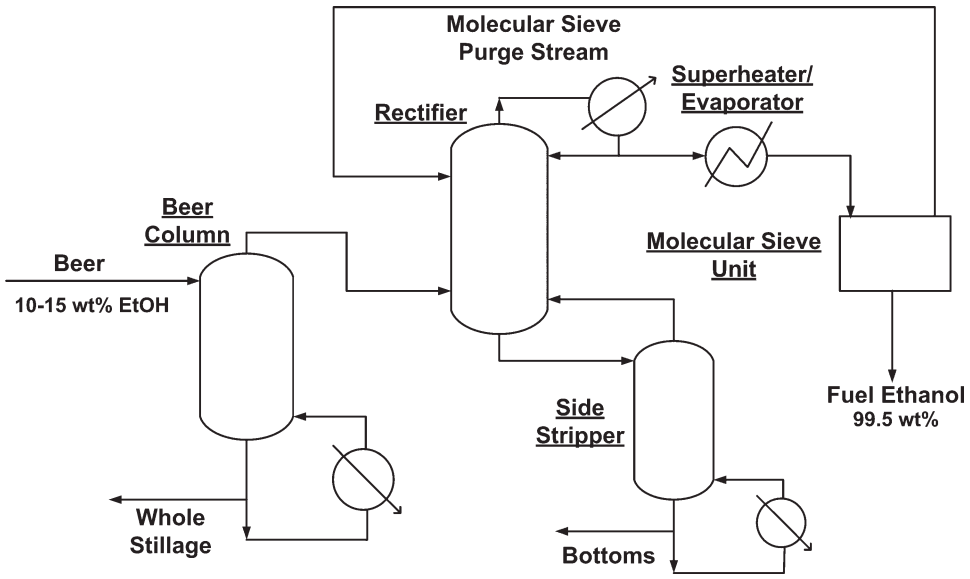

Figure 1. Process flow scheme for ethanol recovery and purification in a state of the art fermentation based corn-to-fuel ethanol plant.

from the fermentation broth and further purification to fuel grade is achieved by three distillation columns (beer column, rectifier, and side stripper) and final water removal by molecular sieve based adsorption[10,20] as shown in Figure 1. Beer from the fermentation process is fed to the beer column operated as a stripper (no reflux) to produce a vapor distillate with an ethanol concentration of about 55 wt % and a bottom aqueous stream, termed whole stillage, consisting of water, dissolved matter, unfermented solids, oils, and trace amounts of ethanol. Then, the vapor distillate from the beer column is enriched to about 92 wt % ethanol in the rectifier. In the adsorption cycle of the molecular sieve unit, superheated moist ethanol vapor from the rectifier overhead is dehydrated to fuel grade ethanol by the selective adsorption of water, whereas in the desorption cycle, the adsorbent bed is depressurized and purged with dry product ethanol vapors for regeneration. The regeneration stream from the adsorbers is recycled to the rectifier. The side stripper strips residual ethanol from the rectifier bottoms stream and the stripped ethanol vapor stream is returned to the rectifier bottoms, whereas the water from the side stripper bottoms is available for recycling to mash preparation and fermentation.

The rectifier and the side stripper essentially operate as a single column, but they are physically separated to minimize capital cost through the opportunity to have the side stripper with a reduced column diameter compared to the rectifier. In this study, a separation train consisting of a beer column, a rectifier (representing both the rectifier and the side stripper in the state of art installations), and a molecular sieve unit is considered as the benchmark process (Figure 2). Further, the beer column and rectifier are assumed to operate under sub atmospheric pressure conditions, enhancing the relative volatility of ethanol at high ethanol concentration.[50] As the molecular sieve unit requires a superheated vapor feed under pressure (172 kPa) in the adsorption cycle, the rectifier overhead condenser is operated as a total condenser producing a liquid distillate which is pressurized with a pump, and then evaporated and superheated for dehydration in the molecular sieve unit.

Salt extractive process–salt in rectifier only: Case II

The efficient recovery and reuse of salt in salt extractive distillation is of paramount importance in regard to the energy demand, capital cost and process requirements. As separation and recovery of salt from the highly complex beer column bottoms stream would be a formidable challenge, no salt should be added to the beer column. The rectifier deals with a relatively clean feed stream (the beer column distillate) without solids which facilitates salt recovery from the rectifier bottoms stream. Because of the above reason, we opted to purify the beer column distillate in a salt extractive rectifier to fuel grade ethanol, eliminating the need for the molecular sieve unit (Figure 3). The salt extractive rectifier bottoms stream is divided into diluate and concentrate for the electrodialysis process. After receiving the salt from the diluate, the salt enriched in the concentrate stream is recovered by evaporating the remaining water with hot natural gas combustion gases in a co-current spray dryer before recycling to the salt extractive rectifier reflux.

Summary of energy demand comparison approach

Comparing energy demands for different processing schemes is complex. Heat integration interconnects unit operations, and different qualities of energy (second law of thermodynamics based balance, for example, thermal vs. electrical) besides the simple quantity of energy (first law of thermodynamics based balance) impact both economics and environmental issues such as green house gas emissions.

The input data and specified parameters for the system boundaries for Case I (benchmark process, Figure 2) and Case II (salt extractive process, Figure 3) are given, respectively, in Tables 1 and 2. Input in Case I and Case II is an

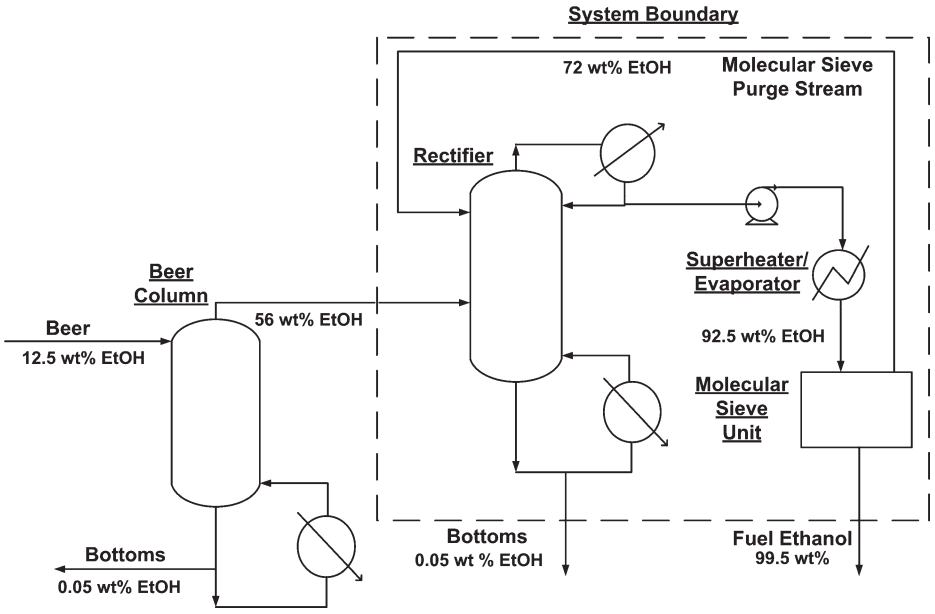

Figure 2. Process flow scheme for Case I—benchmark process.

identical stream of 26.2 tonne/h (vapor distillate containing 56 wt % ethanol and balance water) from a beer column operating as a stripping column at a pressure of 44.8 kPa with 13 stages and a beer feed concentration of 12.5 wt % ethanol, an average of the typical fermentation broth ethanol concentration (about 10–15 wt %) prevalent in contemporary dry mill corn-ethanol facilities. Identical streams of fuel ethanol are produced in Case I and Case II. As an aside, the liquid water output streams from the design cases are not identical as water vapor is lost in the spray dryer with the moist air stream in Case II.

The comparison of the energy demand of Case I and Case II is based on calculating natural gas energy equivalents higher heating value (HHV) for electrical energy or steam that is needed. The thermal energy as steam is converted back to natural gas energy equivalents by using a boiler efficiency of 80%, whereas for electrical energy, a natural gas-to-electrical energy conversion efficiency of 33% was assumed. The thermal energy demand of the spray dryer is directly calculated from the natural gas usage.

Methods

Thermodynamic modeling of the water-ethanol and water-ethanol-$CaCl_2$ systems

The VLE of the water-ethanol system is described by the following equation[52]:

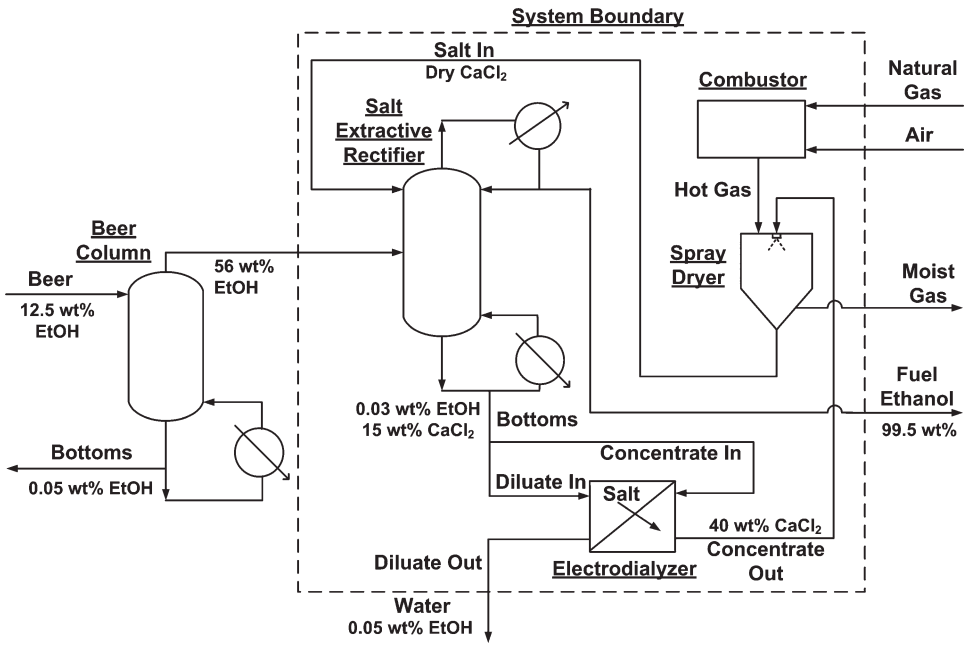

Figure 3. Process flow scheme for Case II—salt extractive process.

Table 1. Input Data and Specified Parameters for Case I—Benchmark Process

Input Data and Specified Parameters	Benchmark Process
Rectifier	
Number of stages	37
Operating pressure (kPa)	34.5
Distillate ethanol concentration (wt %)	92.5
Bottoms ethanol concentration (wt %)	0.05
Molecular sieve unit*	
Operating temperature (K)	389.15
Adsorption pressure (kPa)	172.2
Desorption pressure (kPa)	14.2
Purge stream ethanol concentration (wt %)	72.3
Fuel ethanol concentration (wt %)	99.5

*Data taken from Aden et al.[51]

$$y_i \varphi_i P = x_i \gamma_i P_i^* \varphi_i^* \exp\left[\frac{1}{RT}\int_{p_i^*}^{p} v_i^* dp\right] \quad (1)$$

where y_i and x_i represent, respectively, vapor and liquid phase mole fractions, φ_i and φ_i^* represent partial and pure component fugacity coefficients, respectively, P and P_i^* represent system pressure and pure component vapor pressure in kPa, respectively, γ_i represents the liquid phase activity coefficient, v_i^* represents the saturated liquid molar volume in m^3/kmol at system temperature T in K, and R represents the gas constant in kJ/K kmol. In case of the water-ethanol system, vapor phase fugacity coefficients were calculated using the Redlich-Kwong (RK) equation,[53] whereas liquid phase activity coefficients were calculated using the nonrandom two liquid (NRTL) model.[54] VLE calculations for water–ethanol were performed using default binary parameters (Table 3) in Aspen Properties® 2006.5 for the NRTL-RK property method. The NRTL-RK VLE data shows good agreement with experimental data (Table 4, Figure 4).

In case of the water-ethanol-$CaCl_2$ system, the VLE relationship for the volatile components was determined using Eq. 1. The Redlich-Kwong equation was used to calculate vapor phase fugacity coefficients, and the electrolyte nonrandom two liquid (ENRTL) model[60–62] was used to calculate liquid phase activity coefficients. The ENRTL model assumes that the total excess Gibbs energy (G^{ex}) of the mixed solvent electrolyte system can be represented as a sum of three contributions:

$$G^{ex} = G^{ex}_{PDH} + G^{ex}_{lc} + G^{ex}_{Born} \quad (2)$$

Table 2. Input Data and Specified Parameters for Case II—Salt Extractive Process

Input Data and Specified Parameters	Salt Extractive Process
Salt extractive rectifier	
Number of stages	37
Operating pressure (kPa)	34.5
Distillate ethanol concentration (wt %)	99.5
Bottoms ethanol concentration (wt %)	0.03
Electrodialysis	
Operating temperature (K)	313.15
Concentration of $CaCl_2$ in concentrate (wt %)	40
Current efficiency (%)	90
Spray dryer	
Hot gas temperature (K)	923.15
Moist gas temperature (K)	473.15

Table 3. Binary Parameters of NRTL-RK Property Method for Water (*i*)–Ethanol (*j*) System*

a_{ij}	3.622
a_{ji}	−0.922
b_{ij}	−636.726
b_{ji}	284.286
α_{ij}	0.3

*Molecule–molecule binary parameters were retrieved from Aspen Properties® 2006.5. The energy interaction parameter (τ) was considered as temperature dependent: $\tau_{ij} = a_{ij} + b_{ij}/T$, where T is the system temperature. α_{ij} is the nonrandomness factor.

where G^{ex}_{PDH} represents the long-range interaction contribution from the Pitzer-Debye-Huckel equation, accounting for the electrostatic interactions among the ions. G^{ex}_{lc} represents the short-range interactions among the solution species. These interaction forces are described based on the local composition concept, and on the assumptions of local electroneutrality and like-ion repulsion. G^{ex}_{Born} represents the Born contribution, accounting for the change in Gibbs energy due to the transfer of ionic species from the infinite dilution mixed solvent reference state to the infinite dilution aqueous reference state. The adjustable ENRTL parameters required for water-ethanol-$CaCl_2$ are molecule–molecule (water-ethanol) and molecule-electrolyte (water-$CaCl_2$/ethanol-$CaCl_2$) pair interaction parameters. In the absence of electrolyte components, the ENRTL model reduces to the NRTL model; hence, molecule–molecule pair parameters used in the NRTL model were retained in the ENRTL model. The molecule-electrolyte pair parameters were regressed from experimental data covering the entire range of the process conditions studied (least squares method based on the maximum likelihood principle, DRS module of Aspen Properties® 2006.5). The Britt-Luecke algorithm[63] along with the Deming initialization method was used to regress the pair parameters shown along with other parameters in Table 5. The approach described above showed good agreement with experimental data (Table 6, Figure 4).

Simulation procedure

The distillation columns were rigorously simulated using the MESH equations implemented in the RadFrac module of

Table 4. Deviation Between Experimental Data and NRTL-RK Property Method Calculations for System Temperature (*T*) and Pressure (*P*), and Vapor Phase Mole Fraction of Ethanol (*y*) in Water-Ethanol System

Isobaric VLE			
Pressure (kPa)	ΔT (K)*	Δy*	Refs.
287.5	0.89	0.011	55
101.3	0.11	0.005	56
25.3	–	0.008	57
Isothermal VLE			
Temperature (K)	ΔP (%)†	Δy*	Refs.
343.15	0.43	0.004	58
363.15	0.38	0.004	58

*$\mathrm{AAD} = \sum_{i=1}^{k} \frac{|Z_i - ZM_i|}{k}$, where AAD is the average absolute deviation, Z_i is the regressed property value, ZM_i is the corresponding experimental value, and k is the number of data points.

†$\mathrm{AADP} = \frac{100}{k}\sum_{i=1}^{k}\left|\frac{Z_i - ZM_i}{ZM_i}\right|$, where AADP is the average absolute deviation in percentage, Z_i is the regressed property value, ZM_i is the corresponding experimental value, and k is the number of data points.

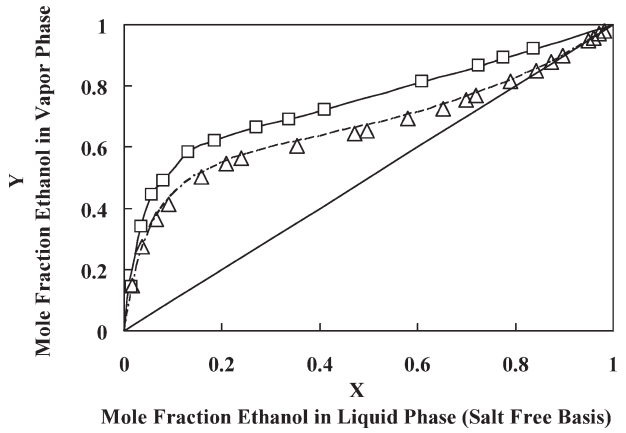

Figure 4. VLE curves for the water-ethanol-$CaCl_2$ and water-ethanol systems: (□) experimental data[59] with 10.8 wt % $CaCl_2$ liquid phase concentration (salt free basis) at 12.3 kPa, (solid line) calculated using ENRTL-RK property method; (Δ) experimental data[57] without salt at 25.3 kPa, (dotted line) calculated using NRTL-RK property method.

Aspen Plus® 2006.5. For the rectifier and the salt extractive rectifier, the Newton algorithm was used, which solves the MESH equations using the Naphtali-Sandholm procedure. Optimum feed stages for the rectifier and the salt extractive rectifier were determined by sensitivity analyses. In Case II, the $CaCl_2$ concentration profile in the salt extractive rectifier is an important parameter. Increasing the $CaCl_2$ concentration in the salt extractive rectifier can decrease the reboiler duty because of the improvement in the VLE, but can lead to an increase in salt recovery energy demand because of the increased $CaCl_2$ mass flow. The $CaCl_2$ concentration in the salt extractive rectifier was optimized to achieve a minimum of the sum of the energy requirements for the system shown in Figure 3. The mass and energy balance calculations for the molecular sieve unit, the electrodialyzer, and the spray dryer were separately performed using Microsoft Excel® 2003 and Mathcad® 13. The results were later incorporated in the overall simulation using the User Model feature of Aspen Plus® 2006.5.

Table 5. Parameters of ENRTL-RK Property Method for Water (*i*)–Ethanol (*j*)–$CaCl_2$ (*k*) System

Dielectric constant of solvents*			
Solvent	*A*	*B*	*C*
Ethanol	24.11	12,601.63	298.15
Water	78.54	31,989.38	298.15

Born radius of ionic species†	
Ionic species	Born radius (10^{-10} m)
Ca^{2+}	1.862
Cl^-	1.937

Molecule-electrolyte binary parameters regressed from experimental data		
Interaction pair	Energy parameter (τ)	Nonrandomness factor (α)
i,*k*	10.262	0.2
k,*i*	−5.160	0.2
j,*k*	29.571	0.0396
k,*j*	−16.093	0.0396

*Values were retrieved from Aspen Properties® 2006.5. The temperature dependency of the dielectric constant (ε) is given by: $\varepsilon = A + B\ (1/T - 1/C)$, where T is the system temperature.
†Values were taken from Rashin and Honig.[64]

Table 6. Deviation Between Experimental Data and ENRTL-RK Property Method Calculations for Osmotic Coefficient (Φ), System Temperature (*T*) and Pressure (P), and Vapor Phase Mole Fraction of Ethanol (*y*) in Water-Ethanol-$CaCl_2$ System

Osmotic coefficients in water-$CaCl_2$ system			
Temperature (K)	Salt concentration (mol/kg solvent)	ΔΦ*	Ref.
298.15	0.1–4	0.058	65

Vapor pressures of water-$CaCl_2$ system			
Temperature (K)	Salt concentration (mol/kg solvent)	ΔP (%)†	Ref.
322.7–398.5	0.957–4.086	0.27	66

Isobaric VLE for water-ethanol-$CaCl_2$ system				
Pressure (kPa)	Salt concentration (mol/kg solvent)	ΔT (K)*	Δ*y**	Ref.
101.3	1.505	0.419	0.004	67
12.3	0.974	0.508	0.001	59

Isothermal VLE for water-ethanol-$CaCl_2$ system				
Temperature (K)	Salt concentration (mol/kg solvent)	ΔP (%)†	Δ*y**	Ref.
298.15	0.474	0.16	0.007	68

*AAD $= \sum_{i=1}^{k} \frac{|Z_i - ZM_i|}{k}$, where AAD is the average absolute deviation, Z_i is the regressed property value, ZM_i is the corresponding experimental value, and k is the number of data points.
†AADP $= \frac{100}{k} \sum_{i=1}^{k} \left|\frac{Z_i - ZM_i}{ZM_i}\right|$, where AADP is the average absolute deviation in percentage, Z_i is the regressed property value, ZM_i is the corresponding experimental value, and k is the number of data points.

Results and Discussion

The target mass flow of fuel grade ethanol to be produced has been fixed (see above) which essentially determines the bottoms mass flow of water from the salt extractive rectifier (Case II), provided there is a negligible ethanol loss with the bottoms. The main parameters are then the reflux (mass flow) in the salt extractive rectifier and the concentration of salt in this reflux stream.

It is necessary to at least eliminate the azeotrope so that fuel grade ethanol can be produced at all in a single salt extractive rectifier. This already occurs at about 2.9 wt % of $CaCl_2$ in the reflux. Above this concentration, the thermal energy demand of the salt extractive rectifier steeply declines with increasing $CaCl_2$ concentration in the reflux but this benefit levels out above about 5 wt % (Figure 5). The reason is that the distillation pinch point, the point of contact between the operating line and the VLE curve in a McCabe-Thiele diagram, shifts from the location at high ethanol content (tangent pinch) to the feed stage (feed pinch) which is

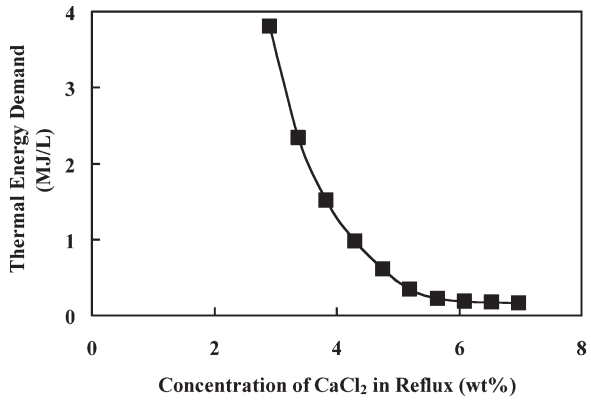

Figure 5. Influence of concentration of $CaCl_2$ in reflux on the thermal energy demand of the salt extractive rectifier.

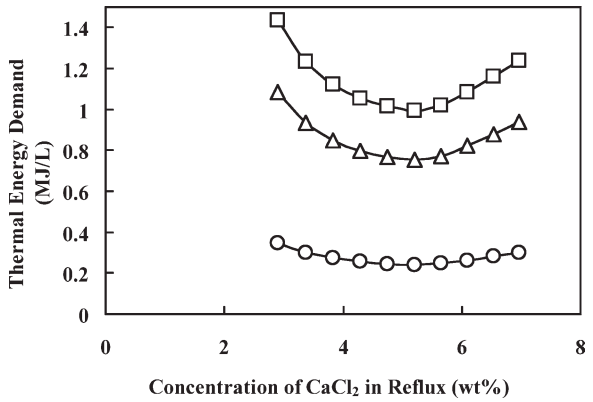

Figure 7. Influence of concentration of $CaCl_2$ in reflux on the thermal energy demand of the salt recovery units: (□) total energy demand, (Δ) spray dryer energy demand, and (○) electrodialyzer energy demand.

at about 56 wt % of ethanol. This shift yields the principal benefit of the salt extractive approach above and beyond eliminating the azeotrope. Further increase in the $CaCl_2$ concentration in the reflux causes an increase in $CaCl_2$ mass flow (Figure 6) along with increasing energy demand for salt recovery (Figure 7) without significant added benefit. The overall combined energy demand, therefore, shows a minimum at about 5.6 wt % $CaCl_2$ in the reflux due to the competition between energy savings due to facilitated distillation, and energy demand for salt recovery (Figure 8). As there is already a large amount of installed capital for corn-based fuel ethanol facilities, the opportunity to improve the already existing process (rectifier and side stripper) by salt extractive distillation is attractive. Matching the salt extractive distillation column diameter and the reboiler and condenser heat transfer areas with that of the corresponding process equipments from Case I is necessary for retrofit purposes. Based on the reflux salt concentrations showing potential energy savings, design calculations indicated salt extractive distillation columns operating with salt concentrations greater than about 5.6 wt % $CaCl_2$ in the reflux satisfy the capacity requirements. An economic analysis (see Appendix) shows at about 6.1 wt % $CaCl_2$ in the reflux, maximal cost savings on the order of 500,000$ per year (Figure 9) can be achieved. Case I requires 1778 kJ/L (6378 Btu/gal) for producing fuel ethanol from the beer column distillate. Retrofitted Case II—salt extractive process, requires 1270 kJ/L (4555 Btu/gal, Figure 10), reducing the thermal energy demand, based on the system boundaries selected here, by 28.5%, which translates to 4.3% thermal energy demand reduction on an overall plant level, considering a fermentation based dry corn mill facility producing both fuel ethanol and DDGS.

Conclusions and Outlook

The approach of fundamentally changing the VLE of water-ethanol mixtures by adding a salt was investigated by process simulation toward energy savings for fermentative fuel ethanol production from corn in a dry mill with DDGS production. Salt extractive distillation, with salt recovery enabled by a new scheme of electrodialysis and spray drying, was conceptually integrated in the water-ethanol separation train of a contemporary fermentation based corn-to-fuel ethanol plant for reducing the thermal energy demand. The VLE of the water-ethanol-$CaCl_2$ system predicted by the ENRTL-RK property method, with the regressed pair parameters,

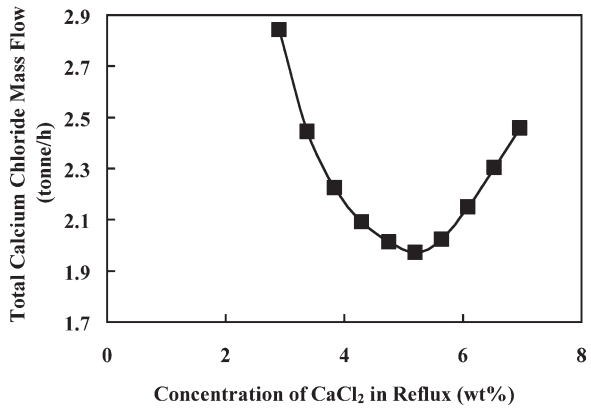

Figure 6. Influence of concentration of $CaCl_2$ in reflux on the total $CaCl_2$ mass flow to the salt extractive rectifier.

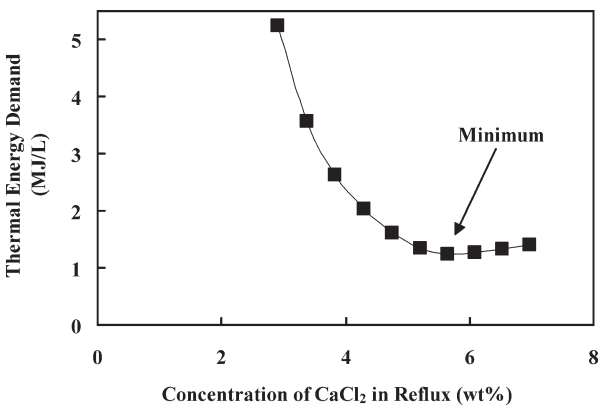

Figure 8. Influence of concentration of $CaCl_2$ in reflux on the total thermal energy demand of the salt extractive rectifier and salt recovery units.

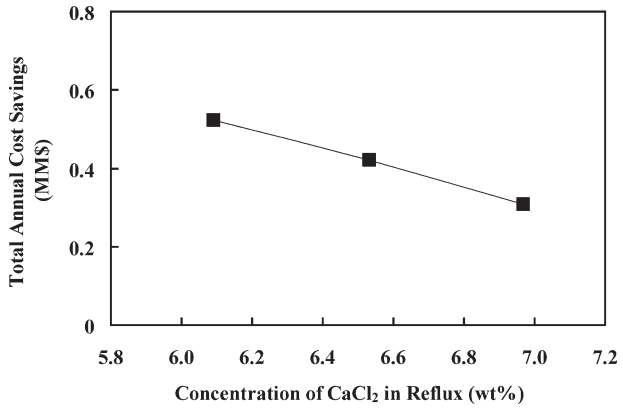

Figure 9. Influence of concentration of $CaCl_2$ in reflux on the total annual cost savings.

showed good agreement with experimental data covering the entire range of process conditions. Retrofitted salt extractive distillation resulted in a thermal energy reduction of 28.5% for producing fuel ethanol from an assumed beer column distillate, if the state of the art rectification/adsorption process (Case I) is compared with the salt extractive rectification with salt recovery (Case II). A thermal energy savings potential of 7.7×10^{13} J (as natural gas HHV) per year with a total annual cost savings potential on the order of $500,000 per year can be estimated for producing 151.4 ML of fuel ethanol (99.5 wt %) per year. An overall maximum energy savings potential of 5.8×10^{16} J or about 0.06 Quad (as natural gas HHV) per year could be realized for the targeted 117.4 GL of fuel ethanol to be produced in the U.S in 2022, if fermentation is the process of choice. The impact of salt extractive distillation on the relatively low ethanol concentrations expected for fermentative cellulosic ethanol production, and the impact of sub-atmospheric pressure distillation will be reported separately along with experimental results.

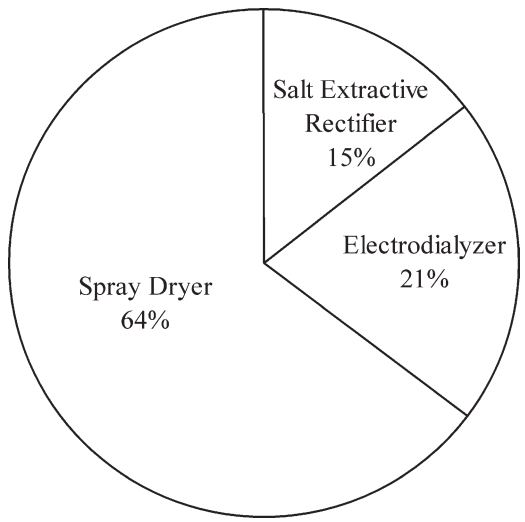

Figure 10. Thermal energy demand distribution of individual process units in retrofitted Case II—salt extractive process (total energy demand: 1270 kJ/L).

Acknowledgments

Support by the U.S. Department of Transportation, the U.S. Department of Energy, and the U.S. Department of Agriculture through the Sun Grant Initiative is gratefully acknowledged (Sub-Award #AB-5-61770-KSU1.01). Support by the Center for Sustainable Energy at Kansas State University is also gratefully acknowledged.

Literature Cited

1. Renewable Fuels Association (RFA). Production capacity of U.S. fuel ethanol plants: operational and under construction/expansion. 2010. Available at: http://www.ethanolrfa.org/bio-refinery-locations/. Accessed May 4, 2010.
2. Graboski MS. *Fossil Energy Use in the Manufacture of Corn Ethanol. Prepared for the National Corn Growers Association*. Denver, CO.: Colorado School of Mines, 2002.
3. Keeney DR, DeLuca TH. Biomass as an energy source for the midwestern U.S. *Am J Altern Agric*. 1992;7:137–144.
4. Lorenz D, Morris D. *How Much Energy Does It Take to Make a Gallon of Ethanol?* Minneapolis, MN: Institute for Local Self-Reliance, 1995.
5. Pimentel D. *Limits of biomass utilization*. In: Meyers RA, editor. *Encyclopedia of Physical Science and Technology, Vol. 2*, 3rd ed. San Diego, U.S.: Academic Press, 2002:159–171.
6. Pimentel D. Ethanol fuels: energy balance, economics, and environmental impacts are negative. *Nat Resour Res*. 2003;12:127–134.
7. Shapouri H, Duffield JA, Graboski MS. *Estimating the Net Energy Balance of Corn Ethanol. Agricultural Economic Report Number 721*. Washington DC: United States Department of Agriculture, 1995.
8. Shapouri H, Duffield JA, Wang M. *The Energy Balance of Corn Ethanol: An Update. Agricultural Economic Report Number 813*. Washington, DC: United States Department of Agriculture, 2002.
9. Eidman VR. Ethanol economics of dry mill plants: chapter 3 in corn-based ethanol in Illinois and the U.S.; a report from the department of agricultural and consumer economics, University of Illinois, November, 2007. Available at: http://www.farmdoc.illinois.edu/policy/research_reports/ethanol_report/index.html. Accessed May 4, 2010.
10. Kwiatkowski JR, McAloon AJ, Taylor F, Johnston DB. Modeling the process and costs of fuel ethanol production by the corn dry-grind process. *Ind Crops Prod*. 2006;23:288–296.
11. Mueller S, Cuttica J. *Research Investigation for the Potential Use of Illinois Coal in Dry Mill Ethanol Plants*. Chicago: Energy Resources Center, University of Illinois, October, 2006. Available at: http://www.chpcentermw.org/12–00_library.html. Accessed May 4, 2010.
12. Wang M, Hong MW, Huo H. Life-cycle energy and greenhouse gas emission impacts of different corn ethanol plant types. *Environ Res Lett*. 2007;2:1–13.
13. Jackson MD, Moyer CB. Alcohol fuels. *Kirk-Othmer Encyclopedia of Chemical Technology: [E-Book]*: NY: Wiley, 2000. Available at: Wiley Online Library. http://onlinelibrary.wiley.com/doi/10.1002/0471238961.0112031510010311.a01/full. Accessed May 4, 2010.
14. Meredith J. *Understanding energy use and energy users in contemporary ethanol plants*. In: Jacques KA, Lyons TP, Kelsall DR, editors. *The Alcohol Textbook*, 4th ed. Thrumpton, U.K.: Nottingham University Press, 2003:355–361.
15. Côté P, Noël G, Moore S. The Chatham demonstration: from design to operation of a 20 m^3/d membrane-based ethanol dewatering system. *Desalination*. 2010;250:1060–1066.
16. Griend DLV. Ethanol distillation process. U.S. Pat. 7,297,236 B1, November 20, 2007.
17. Shapouri H, Gallagher P. *USDA's 2002 Ethanol Cost-of-Production Survey. Agricultural Economic Report Number 841*. Washington, DC: United States Department of Agriculture, 2005.
18. Summers DR, Ehmann D. *Enhanced V-grid trays increase column performance*. Presented at the AIChE Annual Meeting, Indianapolis, IN, November, 2002.
19. Swain RLB. *Molecular sieve dehydrators: why they became the industry standard and how they work*. In: Ingeldew WM, Kelsall DR, Austin GD, Kluhspies C, editors. *The Alcohol Textbook*, 5th ed. Thrumpton, U.K.: Nottingham University Press, 2009:379–384.
20. Vane LM. Separation technologies for the recovery and dehydration of alcohols from fermentation broths. *Biofuels Bioprod Biorefin*. 2008;2:553–588.

21. Côté P, Roy C, Bernier N. Energy reduction in the production of ethanol by membrane dehydration. *Sep Sci Technol.* 2009;44:110–120.
22. Vane LM, Alvarez FR. Membrane-assisted vapor stripping: energy efficient hybrid distillation-vapor permeation process for alcohol-water separation. *J Chem Technol Biotechnol*. 2008;83:1275–1287.
23. Vane LM, Alvarez FR, Huang Y, Baker RW. Experimental validation of hybrid distillation-vapor permeation process for energy efficient ethanol-water separation. *J Chem Technol Biotechnol*. 2010;85:502–511.
24. Karuppiah R, Peschel A, Grossmann IE, Martin M, Martinson W, Zullo L. Energy optimization for the design of corn-based ethanol plants. *AIChE J*. 2008;54:1499–1525.
25. Furter WF. Salt effect in distillation: a technical review. *Chem Eng (Rugby, U. K.).* 1968;46:CE173–CE177.
26. Furter WF. Salt effect in distillation: a literature-review II. *Can J Chem Eng*. 1977;55:229–239.
27. Furter WF. Production of fuel-grade ethanol by extractive distillation employing the salt effect. *Sep Purif Methods*. 1993;22:1–21.
28. Furter WF, Cook RA. Salt effect in distillation—a literature review. *Int J Heat Mass Transfer*. 1967;10:23–36.
29. Cook RA, Furter WF. Extractive distillation employing a dissolved salt as separating agent. *Can J Chem Eng*. 1968;46:119–123.
30. Siklós J, Timár L, Ország I, Ratkovics F. A simulation of the distillation of ethanol-water mixtures containing salts. *Hung J Ind Chem*. 1982;10:309–316.
31. Cespedes AP, Ravagnani SP.Modelado y simulación del proceso de destilacion extractiva salina de etanol. *Inf Tecnol*. 1995;6:17–20.
32. Ligero EL, Ravagnani TMK. Simulation of salt extractive distillation with spray dryer salt recovery for anhydrous ethanol production. *J Chem Eng Jpn*. 2002;35:557–563.
33. Ligero EL, Ravagnani TMK. Dehydration of ethanol with salt extractive distillation—a comparative analysis between processes with salt recovery. *Chem Eng Process*. 2003;42:543–552.
34. Lynd LR, Grethlein HE. IHOSR/Extractive distillation for ethanol separation. *Chem Eng Prog*. 1984;80:59–62.
35. Schmitt D, Vogelpohl A. Distillation of ethanol - water solutions in the presence of potassium acetate. *Sep Sci Technol.* 1983;18:547–554.
36. Ravagnani SP, Reis PR. Modelo de orden reducido aplicado a una columna de destilacion extractiva salina. *Inf Tecnol*. 2000;11:43–50.
37. Torres JL, Grethlein HE, Lynd LR. Computer simulation of the Dartmouth process for separation of dilute ethanol water mixtures. *Appl Biochem Biotechnol*. 1989;20:621–633.
38. Barba D, Brandani V, Digiacomo G. Hyperazeotropic ethanol salted-out by extractive distillation—theoretical evaluation and experimental check. *Chem Eng Sci*. 1985;40:2287–2292.
39. Llano-Restrepo M, Aguilar-Arias J. Modeling and simulation of saline extractive distillation columns for the production of absolute ethanol. *Comput Chem Eng*. 2003;27:527–549.
40. Pinto RTP, Wolf-Maciel MR, Lintomen L. Saline extractive distillation process for ethanol purification. *Comput Chem Eng*. 2000;24:1689–1694.
41. Elander RT, Putsche VL. *Ethanol from corn: technology and economics*. In: Wyman CE, editor. *Handbook on Bioethanol: Production and Utilization.* Washington, DC: Taylor & Francis; 1996:329–349.
42. Kelsall DR, Piggot R. *Grain milling and cooking for alcohol production: designing for the options in dry milling*. In: Ingeldew WM, Kelsall DR, Austin GD, Kluhspies C, editors. *The Alcohol Textbook*, 5th ed. Thrumpton, U.K.: Nottingham University Press, 2009:161–175.
43. Russell I. *Understanding yeast fundamentals*. In: Jacques KA, Lyons TP, Kelsall DR, editors. *The Alcohol Textbook*, 4th ed. Thrumpton, U.K.: Nottingham University Press, 2003:85–119.
44. Seader JD, Henley EJ. *Separation Process Principles*, 2nd ed. New York: Wiley, 2006.
45. Sata T. *Ion Exchange Membranes: Preparation, Characterization, Modification and Application.* Cambridge, U.K.: Royal Society of Chemistry, 2004.
46. Strathmann H. *Ion-Exchange Membrane Separation Processes*, 1st ed. Amsterdam, The Netherlands: Elsevier, 2004.
47. Pfromm PH. Low effluent processing in the pulp and paper industry: electrodialysis for continuous selective chloride removal. *Sep Sci Technol*. 1997;32:2913–2926.
48. Masters K. *Spray Drying Handbook*, 4th ed. London: George Godwin, 1985.
49. Oakley DE. Spray dryer modeling in theory and practice. *Drying Technol*. 2004;22:1371–1402.
50. Maiorella B, Wilke CR, Blanch HW. *Alcohol production and recovery*. In: Fiechter A, editor. *Advances in Biochemical Engineering*, Vol. 20. Berlin: Springer-Verlag, 1981:43–92.
51. Aden A, Ruth M, Ibsen K, Jechura J, Neeves K, Sheehan J, Wallace B, Montague L, Slayton A, Lukas J. Lignocellulosic Biomass to Ethanol Process Design and Economics Utilizing Co-current Dilute Acid Prehydrolysis and Enzymatic Hydrolysis for Corn Stover, NREL/TP-510–32438. NREL, Golden, CO, 2002.
52. Aspen Technology, Inc. *Aspen Physical Property System—Physical Property Methods, Ver. 2006.5*. Cambridge, MA: Aspen Technology, Inc., 2007.
53. Redlich O, Kwong JNS. On the thermodynamics of solutions. V. An equation of state. Fugacities of gaseous solutions. *Chem Rev (Washington, DC, U. S.).* 1949;44:233–244.
54. Renon H, Prausnitz JM. Local compositions in thermodynamic excess functions for liquid mixtures. *AIChE J*. 1968;14:135–144.
55. Othmer DF, Moeller WP, Englund SW, Christopher RG. Composition of vapors from boiling binary solutions—recirculation-type still and equilibria under pressure for ethyl alcohol-water system. *Ind Eng Chem.* 1951;43:707–711.
56. Kurihara K, Nakamichi M, Kojima K. Isobaric vapor-liquid-equilibria for methanol+ethanol+water and the 3 constituent binary-systems. *J Chem Eng Data*. 1993;38:446–449.
57. Beebe AH Jr, Coulter KE, Lindsay RA, Baker EM. Equilibria in ethanol-water system at pressures less than atmospheric. *Ind Eng Chem.* 1942;34:1501–1504.
58. Pemberton RC, Mash CJ. Thermodynamic properties of aqueous non-electrolyte mixtures. 2. Vapor-pressures and excess Gibbs energies for water+ethanol at 303.15-K to 363.15-K determined by an accurate static method. *J Chem Thermodyn.* 1978;10:867–888.
59. Meyer T, Polka HM, Gmehling J. Low-pressure isobaric vapor-liquid-equilibria of ethanol water mixtures containing electrolytes. *J Chem Eng Data*. 1991;36:340–342.
60. Chau-Chyun C, Britt HI, Boston JF, Evans LB. Local composition model for excess Gibbs energy of electrolyte systems, part I. Single solvent, single completely dissociated electrolyte systems. *AIChE J*. 1982;28:588–596.
61. Chen CC, Evans LB. A local composition model for the excess Gibbs energy of aqueous-electrolyte systems. *AIChE J*. 1986;32:444–454.
62. Mock B, Evans LB, Chen CC. Thermodynamic representation of phase-equilibria of mixed-solvent electrolyte systems. *AIChE J*. 1986;32:1655–1664.
63. Britt IH, Luecke RH. The estimation of parameters in nonlinear, implicit models. *Technometrics*. 1973;15:233–247.
64. Rashin AA, Honig B. Reevaluation of the Born model of ion hydration. *J Phys Chem.* 1985;89:5588–5593.
65. Robinson RA, StokesRH. *Electrolyte Solutions*, 2nd ed. London: Butterworths, 1970.
66. Sako T, Hakuta T, Yoshitome H. Vapor-pressures of binary (H_2O-Hcl, H_2O-$MgCl_2$, and H_2O-$CaCl_2$) and ternary (H_2O-$MgCl_2$-$CaCl_2$) aqueous-solutions. *J Chem Eng Data*. 1985;30:224–228.
67. Nishi Y. Vapor-liquid equilibrium relations for the system accompanied by hypothetical chemical reaction containing salt. *J Chem Eng Jpn*. 1975;8:187–191.
68. Mishima K, Iwai Y, Yamaguchi S, Isonaga H, Arai Y, Hongo M. Correlation of vapor—liquid equilibria of ethanol-water-calcium chloride and methanol-ethanol-calcium chloride systems at 25°C. *Mem Facul Eng Kyushu Univ*. 1986;46:407–433.

Appendix

Aspen Icarus Process Evaluator® 2006.5 was used to estimate all process equipment cost except for molecular sieve units and the electrodialyzer. In this study, the costs (US$ basis) were updated using chemical engineering plant cost index (CEPCI) and are reported on 2010 second quarter basis. Molecular sieve equipment cost was estimated using the scaling and installation factors taken from Aden et al.,[51] whereas the electrodialyzer equipment cost was estimated using the following equations:

$$C_{EDZ} = C_P + C_S \quad \text{(A1)}$$

$$C_P = 1.5 \times C_S \quad \text{(A2)}$$

$$C_S = 1.5 \times (2M_A) \times C_M \quad \text{(A3)}$$

$$M_A = \frac{ZFn_s}{\eta i_{cd}} \quad \text{(A4)}$$

where C_{EDZ} is the electrodialyzer installed equipment cost, C_P and C_S are the peripheral and stack costs, respectively, M_A is the overall membrane area required for each ion exchange membrane type (m^2), Z is the ion valence (equivalent/mol), F is the Faraday constant (96485 A s/equivalent), n_s is the salt removal rate (mol/s), η is the electrical current efficiency, and i_{cd} is the operating current density (A/m^2). The following values were used:

$C_M = \$100/m^2$

$\eta = 0.9$

$i_{cd} = 300\ A/m^2$

To calculate the annual operating costs (C_O), a plant operation time of 7920 h/year, and the following utility costs were used: steam—\$17.08/tonne, cooling water—\$0.07/tonne, process water—\$0.53/tonne, electricity—\$0.07/kW h, and natural gas—\$5.7/GJ (\$6/MM Btu).

The total annualized cost (TAC) was calculated using the following equations:

$$TAC = C_O + ACCR \times TIC \quad \text{(A5)}$$

$$ACCR = \frac{i(1+i)^n}{(1+i)^n - 1} \quad \text{(A6)}$$

where ACCR is the annual capital charge ratio, TIC is the total installed equipment cost, i is the interest rate, and n is the plant life (years). The following values were used:

$i = 0.1$

$n = 10$ years (general plant life)

$n = 5$ years (for membrane replacement cost)

Finally, the total annual cost savings (TACS) was calculated using the following equation:

$$TACS = TAC_{CaseI} - TAC_{CaseII} \quad \text{(A7)}$$

Manuscript received Aug. 27, 2010, and revision received Jan. 14, 2011.